The Sensitivity of Ice Cloud Optical and Microphysical Passive Satellite Retrievals to Cloud Geometrical Thickness

Gang Hong, Ping Yang, Hung-Lung Huang, Bryan A. Baum, Yongxiang Hu, and Steven Platnick

***Abstract*—Most satellite-based ice cloud retrieval algorithms rely on precomputed lookup libraries for inferring the ice cloud optical thickness (τ) and effective particle size (D_e). However, this retrieval methodology does not account for the case where cloud geometrical thickness may vary by several kilometers. In this paper, we investigate the effect of the ice cloud geometrical thickness on the retrieval of τ and D_e for algorithms using the Moderate Resolution Imaging Spectroradiometer infrared (IR) bands at 8.5 and 11 μm (or 12 μm) or solar bands at 0.65 and 1.64 μm (or 2.13 μm). We use a rigorous radiative transfer package to simulate the IR brightness temperatures and solar reflectances, assuming that the ice cloud top height is fixed at 12 or 15 km with a variation of cloud geometrical thickness from 0.5 to 5 km. The simulated brightness temperatures and reflectances are then used to investigate the errors of cloud τ and D_e inferred from the precomputed lookup tables developed with a specific geometrical thickness. It is found that the retrieval errors in τ and D_e increase with increasing τ for the IR and solar methods. In both cases, cloud τ and D_e may be underestimated and overestimated, respectively, if the effect of the cloud geometrical thickness is not taken into account. The effect of the cloud geometrical thickness on the retrieval of cloud optical and microphysical properties is much larger for the IR algorithm than for the solar-band-based algorithm. This paper demonstrates that the inclusion of the information about the cloud geometrical thickness may improve the accuracy of the retrieval of the cloud properties on the basis of the precomputed lookup libraries.**

***Index Terms*—Geometrical thickness, ice cloud, Moderate Resolution Imaging Spectroradiometer (MODIS), remote sensing.**

I. Introduction

ICE CLOUDS are ubiquitous [1]–[4] and play an important role in the climate system through their effects on the radiation budget [5]. Currently, ice clouds are a source of substantial uncertainties in satellite and modeling studies [1], [6]–[10], and several field campaigns (see e.g., [11] and [12]) were dedicated to a better understanding of the ice cloud's properties. The effects of ice clouds on climate are highly sensitive to the optical and microphysical properties of these clouds [6]. Baker [13] found that variations of ice cloud amount can lead to differences of up to 17 $W \cdot m^{-2}$ in the globally averaged radiation flux entering or leaving the terrestrial atmosphere.

The optical and microphysical properties of ice clouds can be inferred from the solar reflectance measurements in visible through midwave infrared spectral bands [9], [14]–[19]. In general, the spectral bands centered at 1.6, 2.1, and 3.7 μm are sensitive to the cloud effective particle size (D_e), whereas the nearly nonabsorbing bands centered at 0.65, 0.86, and 1.2 μm are primarily sensitive to the cloud optical thickness (τ). A combination of two bands with significantly different cloud particle absorption can be used to simultaneously retrieve cloud τ and D_e [15], [16], [18]. In addition to solar-reflectance algorithms, infrared (IR) bands at 8.5, 11, and 12 μm are often used and have the advantage of being independent of solar illumination. Stubenrauch *et al.* [20] and Rädel *et al.* [21] retrieved the cirrus cloud D_e using the difference of cirrus spectral emissivities at the 8- and 11-μm wavelengths. The split window bands (11 and 12 μm) have also been used to estimate τ and D_e for cirrus and contrail [7], [22]–[25]. These retrieval algorithms are essentially based on the precomputed lookup tables of reflectances or brightness temperatures. Specially, cirrus τ and D_e are determined by searching the tables for entries that minimize the difference in comparison with measurements [16], [20], [25], [26].

Extensive sensitivity studies have been carried out to understand the limitations of the retrieval techniques and the assumptions inherent to the methods [15]–[17], [20]–[29]. However, little effort has been carried out to understand the uncertainties pertaining to the cloud geometrical thickness. Rädel *et al.* [21] showed that the effect of the cloud geometrical thickness on D_e retrieved from the 8- and 11-μm bands is on the order of a few percent with the maximum error of 10% when the cirrus geometrical thickness varies between 1 and 2 km. Using 35-GHz radar observations over the U.S. DOE Atmospheric Radiation Measurement Program's Southern Great Plains site, Luo *et al.* [30] found that the cirrus geometrical thickness can be up to 8 km. The intent of this paper is to understand the uncertainties in the retrieval of cirrus τ and D_e, pertaining to

Manuscript received June 5, 2006; revised February 2, 2007. This work was supported in part by a NASA research grant (NNG04GL24G) from NASA Radiation Sciences Program managed by Dr. Hal Maring (previously by Dr. Donald Anderson) and the MODIS Program managed by Dr. Paula Bontempi, and in part by the National Science Foundation Physical Meteorology Program (ATM-0239605) managed by Dr. Andrew Detwiler.

G. Hong and P. Yang are with the Department of Atmospheric Sciences, Texas A&M University, College Station, TX 77843 USA (e-mail: pyang@ariel.met.tamu.edu).

H.-L. Huang and B. A. Baum are with the Space Science and Engineering Center, University of Wisconsin-Madison, Madison, WI 53706 USA.

Y. Hu is with the NASA Langley Research Center, Hampton, VA 23681 USA.

S. Platnick is with the Earth Sciences Division, NASA Goddard Space Flight Center, Greenbelt, MD 20771 USA.

Digital Object Identifier 10.1109/TGRS.2007.894549

the neglect of the geometrical thickness of the clouds in the retrieval.

The rest of this paper is organized as follows. Section II describes the radiative transfer model used in this paper for simulating the IR brightness temperatures and the bidirectional reflectances. The effect of the cloud geometrical thickness on the simulated brightness temperatures and bidirectional reflectances is discussed in Section III. Section IV presents an error analysis regarding the effect of the cloud geometrical thickness on the retrieval of τ and D_{e}. Conclusions are given in Section V.

II. Data and Radiative Transfer Models

In this paper, we consider three IR bands centered at 8.5, 11, and 12 μm and three solar bands centered at 0.65, 1.64, and 2.13 μm. The single-scattering properties of individual ice particles are taken from [31] and [32] for the solar bands and the IR bands, respectively. An ice cloud is assumed to consist of 50% bullet rosettes, 25% hexagonal plates, and 25% hollow columns for small ice particles when the maximum dimensions of the ice particles are smaller than 70 μm, and 30% aggregates, 30% bullet rosettes, 20% hexagonal plates, and 20% hollow columns when the maximum dimensions of the ice particles are larger than 70 μm, following the studies in [9] and [32]–[35]. To compute the bulk single-scattering properties of the ice clouds, we use the size distributions compiled by Fu [36] and Mitchell *et al.* [37].

The optical thicknesses for each layer in a clear-sky atmosphere are computed with a set of correlated k-distribution routines developed to account for the atmospheric molecular absorption. The correlated k-distribution routines have been tailored specifically to the Moderate Resolution Imaging Spectroradiometer (MODIS) bands used in this paper [9], [33], [38], [39]. The tropical standard atmosphere vertical profiles of temperature, pressure, water vapor, and ozone are used in the correlated k-distribution calculations. The profiles of other trace gases are assumed to have constant mixing ratios at each level. The atmosphere is divided into 100 layers from the surface to 100 km and with a vertical resolution of 0.5 km below 30 km. The cloud temperature is assumed to be the same as the atmospheric temperature at the corresponding level; surface temperature is set equal to the lowest atmospheric layer. The surface emissivity is assumed to be 0.98 for the IR bands, whereas the surface albedo is assumed to be 0.2 for the solar bands.

A single-layered ice cloud with a cloud top of 12 or 15 km and a constant D_{e} is used for the present sensitivity study. The geometrical thickness of the cloud is assumed to be 0.5, 1, 3, or 5 km. Furthermore, we assume that τ varies from 0 to 80 and that D_{e} interpolated on the basis of the size distributions compiled by Fu [36] and Mitchell *et al.* [37] varies from 8 to 96 μm. The IR brightness temperatures at the top of atmosphere (TOA) are computed for a nadir-viewing geometry (satellite zenith angle $\theta = 0^{\circ}$). For simulating the bidirectional reflectances, the solar zenith angle θ_0, satellite zenith angle θ, and relative azimuth angle ϕ are set to 30°, 0°, and 90°, respectively. The brightness temperatures at 8.5, 11, and 12 μm and the reflectance functions at 0.65, 1.64, and 2.13 μm are calculated at the top of the atmosphere using the discrete ordinates radiative transfer model (DISORT) code [40].

III. Effect of Cloud Geometrical Thickness on Brightness Temperatures and Reflectances

Fig. 1 shows the effect of cloud geometrical thickness on the simulated brightness temperatures at 8.5, 11, and 12 μm for an optically thick ice cloud ($\tau = 10$) with a fixed cloud top height of 12 or 15 km above the surface. For reference, we use the simulated results associated with a cloud geometrical thickness of 0.5 km. The effect of cloud geometrical thickness on the brightness temperatures is indicated by the relative changes in brightness temperatures ($\Delta T/T$) for the simulated results assuming geometrical thicknesses of 1, 3, and 5 km with respect to the reference cloud geometrical thickness of 0.5 km. The results are similar for all the bands (Fig. 1), but the influence is stronger for the 8.5- and 11-μm bands than for the 12-μm band. The cloud top height has a weak influence on $\Delta T/T$. When the cloud geometrical thickness is small (1 km), the effect of the cloud geometrical thickness is independent of D_{e}. For the 8.5- and 11-μm bands, the effect of cloud geometrical thickness reaches its asymptotic value with respect to the increase of D_{e}.

Fig. 2 shows $\Delta T/T$ for a cloud for which D_{e} is fixed at 56 μm and τ varies from 0 to 80. The effect of the cloud geometrical thickness on the brightness temperatures depends strongly on τ. The largest effect is observed when τ ranges between 5 and 9 for all the bands. When $\tau < 5$, $\Delta T/T$ increases sharply with decreasing τ. When $\tau > 5$, $\Delta T/T$ decreases with increasing τ. Again, the cloud top height has a weak influence on $\Delta T/T$.

The effects of the cloud geometrical thickness on the bidirectional reflectances at the 0.65-, 1.64-, and 2.13-μm bands are investigated in the same way as in the case of the IR bands. Fig. 3 shows the relative changes ($\Delta R/R$) in reflectance differences as functions of D_{e} when $\tau = 10$. The bidirectional reflectances for the three bands have similar features. $\Delta R/R$ increases with increasing cloud geometrical thickness. The influence of the cloud geometrical thickness at the 0.65-μm band has a weaker dependence on D_{e} in comparison with the 1.64- and 2.13-μm bands. The effect in the 1.64-μm band is approximately two times larger than for the 2.13-μm band. The variations in cloud top height have a stronger influence on $\Delta R/R$ for the 1.64-μm band than for the 0.65- and 2.13-μm bands.

Fig. 4 shows the effect of the cloud geometrical thickness on the bidirectional reflectances as functions of τ when $D_{\mathrm{e}} = 56$ μm. Similar to the results shown in Fig. 3, the influence on the reflectances increases with the geometrical thickness. The 1.64- and 2.13-μm reflectances have similar features, although the influence of the geometrical thickness for the 1.64-μm band is approximately two times larger than for the 2.13-μm band when τ is smaller than 10 [Fig. 4(b) and (c)]. As τ increases, the relative changes in reflectances at the 0.65-μm band increase and approach an asymptotic value. Different from the 0.65-μm band, the relative changes in reflectances for the

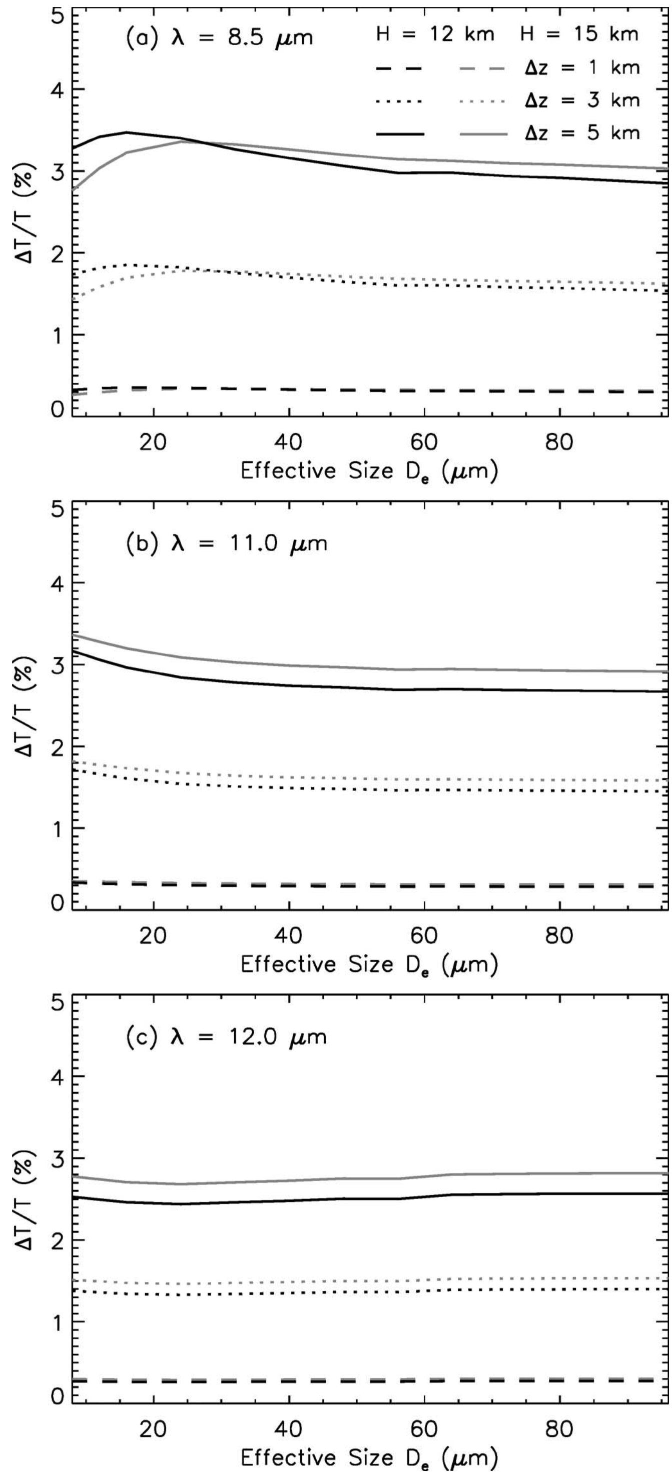

Fig. 1. Relative changes in brightness temperatures $(\Delta T/T)$ computed with respect to a reference cloud geometrical thickness of 0.5 km. Cloud optical thickness is fixed at 10 km and cloud top height is fixed at 12 or 15 km, respectively.

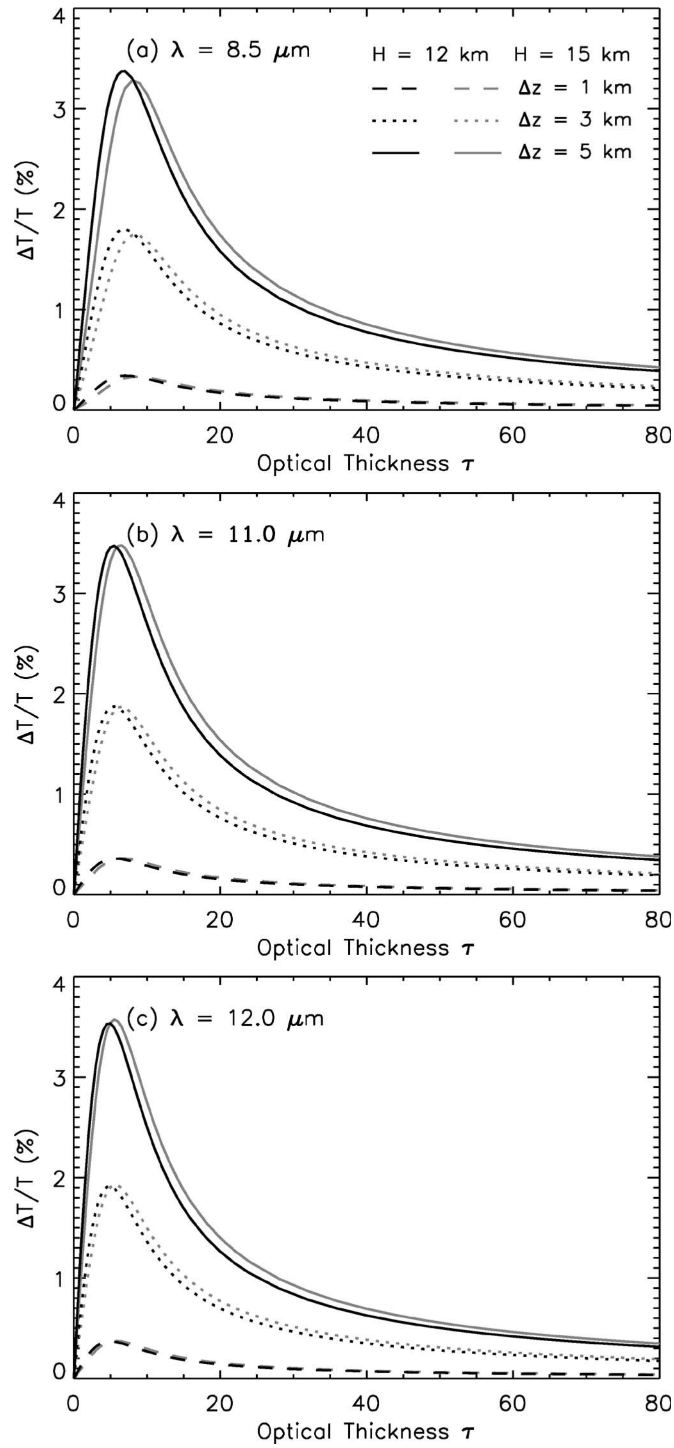

Fig. 2. Same as in Fig. 1, except that the effect of cloud geometrical thickness as a function of optical thickness is shown.

1.64- and 2.13-μm bands first increase sharply for small τ values, then decrease sharply for τ in the range of 5–30 and, eventually, reach an asymptotic value that is different from that of the reference case [Fig. 4(b) and (c)]. Similar to the case in Fig. 3, the effect of the cloud top height on $\Delta R/R$ is stronger for the 1.64-μm band than for the 0.65- and 2.13-μm bands.

IV. Effect of Cloud Geometrical Thickness on the Retrieval of τ and D_{e}

To understand how the variations in the cloud geometrical thickness affect the retrieval of D_{e} and τ, precomputed lookup tables are derived for the IR bands at 8.5 and 11 μm and the solar bands at 0.65 and 1.64 μm. Simulations for an ice cloud with a geometrical thickness of 0.5 km and a cloud top height at 12 or 15 km are carried out to develop the lookup

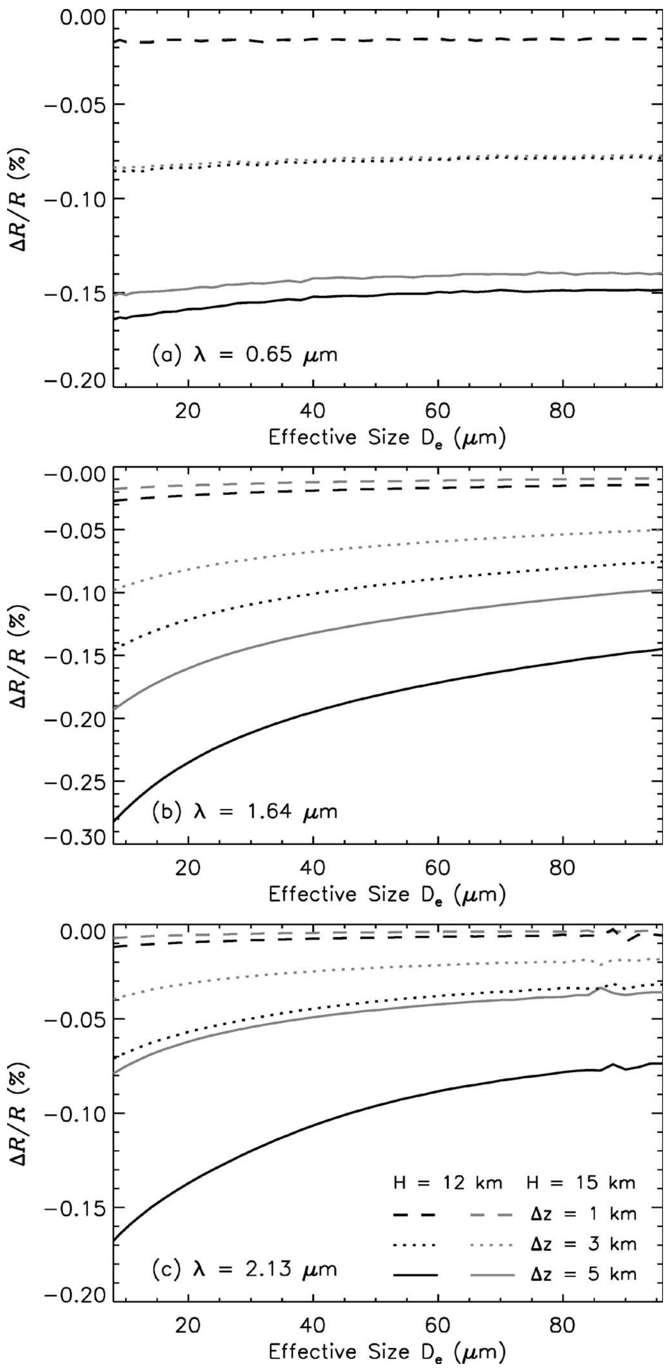

Fig. 3. Relative changes in bidirectional reflectances ($\Delta R/R$) computed with respect to a reference cloud geometrical thickness of 0.5 km. Cloud optical thickness is fixed at 10 km and cloud top height is fixed at 12 or 15 km, respectively.

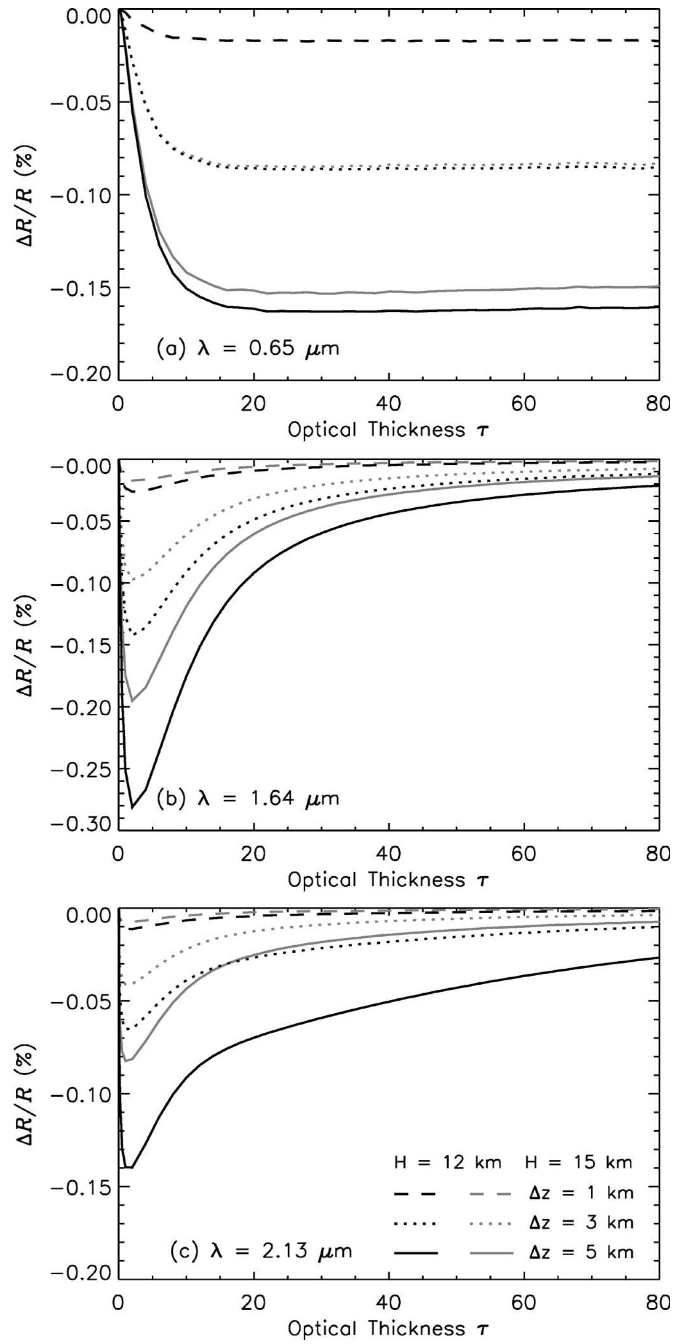

Fig. 4. Same as in Fig. 3, except that the effect of cloud geometrical thickness as a function of optical thickness is shown.

tables. Based on these calculations for a reference cloud, Fig. 5 shows the simulated brightness temperatures at 8.5 and 11 μm [Fig. 5(a)] and the bidirectional reflectances at the 0.65- and 1.64-μm bands [Fig. 5(b)]. The lookup tables with a cloud top height at 12 or 15 km have similar features; therefore, here, only the lookup tables with a cloud top height at 12 km are shown. To show the effect of the cloud geometrical thickness on the retrieval of τ and D_{e}, the lookup tables for an ice cloud with a geometrical thickness of 5 km are also shown in comparison with the lookup tables for the ice cloud with the reference geometrical thickness of 0.5 km. Since the IR brightness temperatures are insensitive to τ when its value is larger than approximately 10 [41], the present sensitivity study focuses on the case of $\tau < 10$. The retrievals based on the IR band lookup tables are influenced more by the variations in ice cloud geometrical thickness [Fig. 5(a)] than are those for the solar bands [Fig. 5(b)].

The retrieval of τ and D_{e} using the two IR bands [Fig. 5(a)] is equivalent to minimizing the error χ^2 defined as

$$\chi^2 = \left[T_8^s(\theta) - T_8^t(\tau, D_{\mathrm{e}}; \theta)\right]^2 + \left[T_{11}^s(\theta) - T_{11}^t(\tau, D_{\mathrm{e}}; \theta)\right]^2 \tag{1}$$

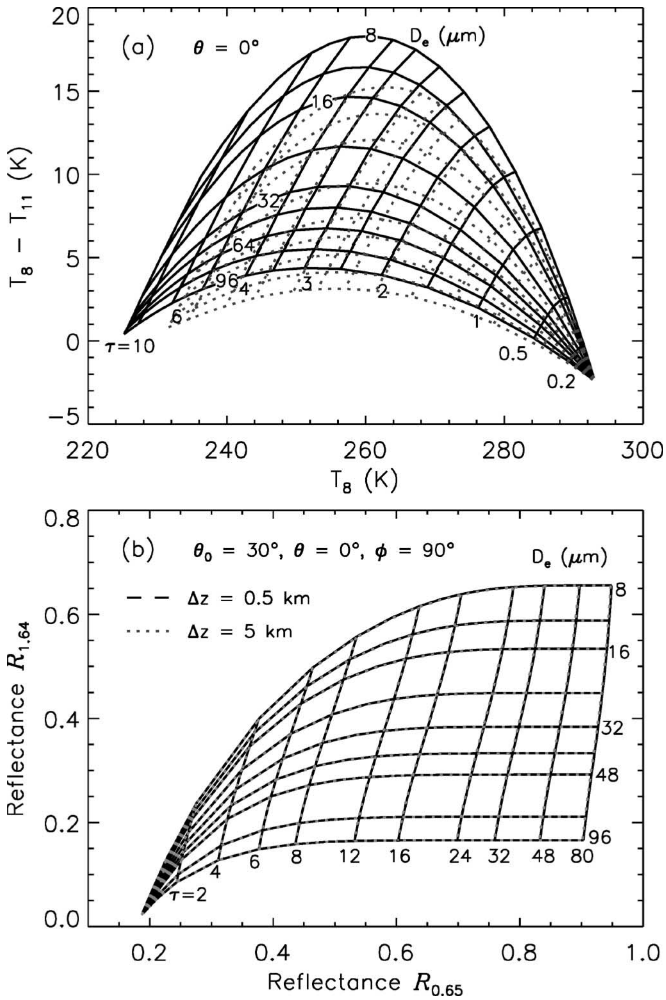

Fig. 5. (a) Relationship between the brightness temperature difference between 8.5 and 11 μm and the brightness temperature at 8.5 μm for various values of ice cloud optical thickness and effective particle size when $\theta = 0°$. (b) The relationship between the reflectance function at 0.65 and 1.64 μm for various values of ice cloud optical thickness and effective particle size when $\theta_0 = 30°$, $\theta = 0°$, and $\phi = 90°$. Ice cloud top height is fixed at 12 km. Ice cloud geometrical thickness is set to be 0.5 km for a reference and 5.0 km, respectively.

where T_8^s and T_{11}^s are the simulated brightness temperatures at the 8.5- and 11.0-μm bands, respectively; T_8^t and T_{11}^t are the brightness temperatures in the lookup tables. The satellite viewing angle θ is 0° (i.e., at nadir). From this minimization procedure, the retrieved τ and D_e can be obtained.

Similar radiative transfer calculations are carried out for an ice cloud with a cloud top height at 12 or 15 km but with geometrical thicknesses of 1, 3, and 5 km. These simulated values are used in turn to infer ice cloud τ and D_e based on the lookup table for the reference cloud with a geometrical thickness of 0.5 km. The relative error of the retrieval is defined as the ratio of the retrieval difference (i.e., the retrieved values minus the true values) to the true value. Fig. 6 shows the relative retrieval errors as a function of τ for D_e values of 16, 56, and 96 μm. Note that τ is plotted in a logarithmic scale to better delineate the differences when τ is small. An increase in cloud geometrical thickness leads to an underestimation in the retrieved τ. Retrieval errors increase for a given τ as the

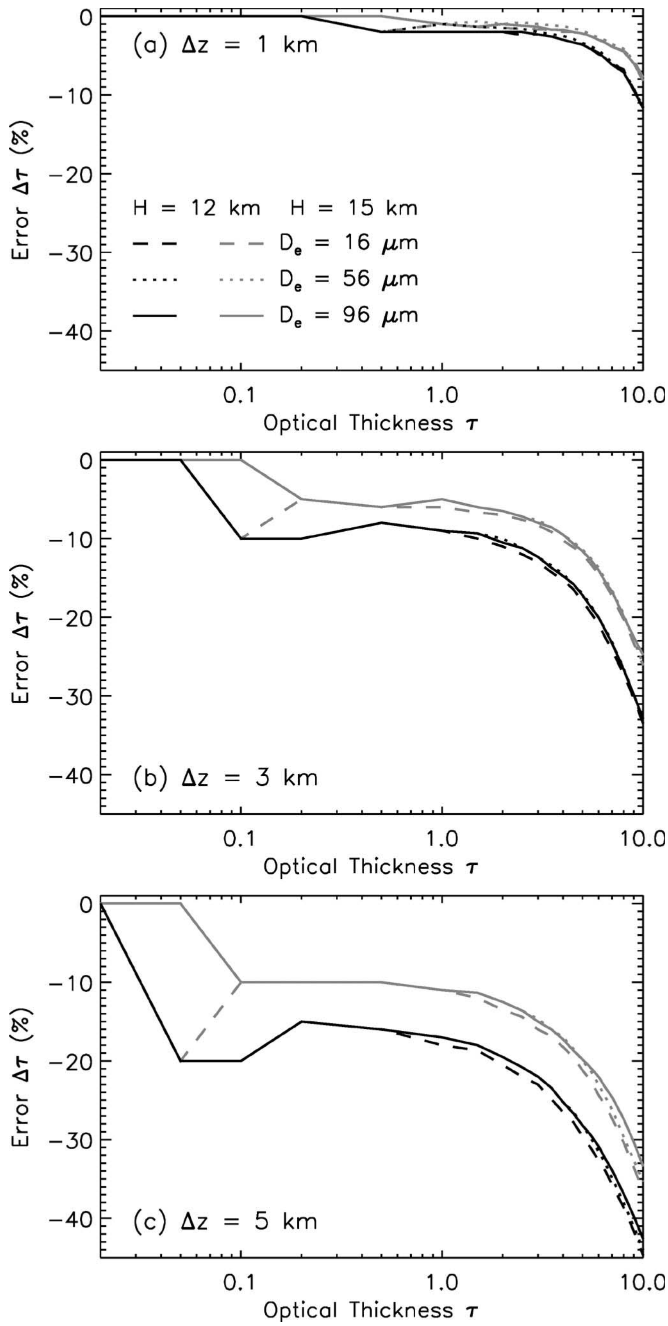

Fig. 6. Relative error $\Delta\tau(\%)$ in the retrieved optical thickness for three values of ice cloud geometrical thicknesses (1, 3, and 5 km) based on the IR simulations shown in Fig. 5(a).

cloud geometrical thickness increases. A general result is that the retrieval errors for τ seem to be independent of D_e.

The relative errors for the retrieved D_e as a function of cloud reference D_e and for τ of 0.1, 1, or 10 using the IR bands are shown in Fig. 7. The increase of cloud geometrical thickness leads to an overestimation in the retrieved cloud D_e. Moreover, the errors increase with increasing cloud geometrical thickness. The largest errors occur for the largest values of τ. When τ is small (< 1), the errors slightly vary with cloud D_e. However, when τ is large (> 1), the errors depend strongly on D_e. Both the relative retrieval errors of τ and D_e are sensitive to the cloud top height (Figs. 6 and 7).

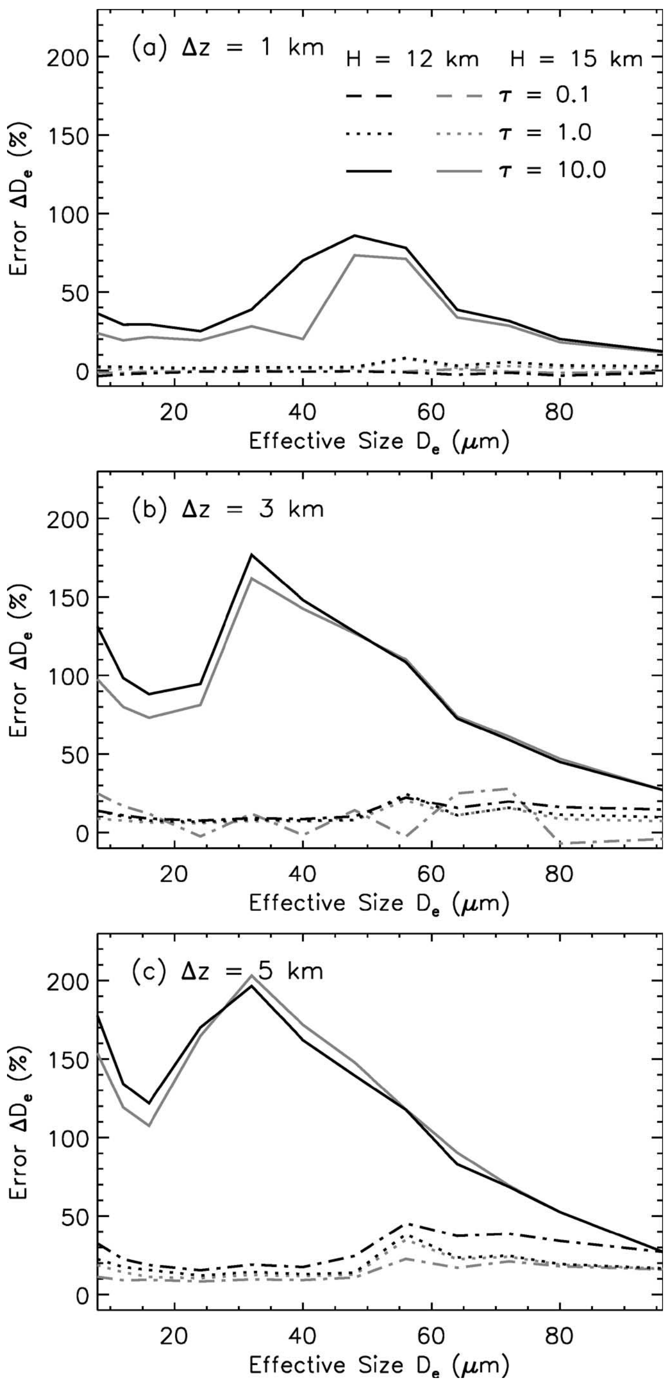

Fig. 7. Relative error $\Delta D_{\mathrm{e}}(\%)$ in the retrieved particle effective size for three ice cloud geometrical thicknesses (1, 3, and 5 km) based on the IR simulations shown in Fig. 5(a).

Similar to (1), the retrieval of τ and D_{e} from the lookup tables for the solar bands is equivalent to minimizing the error χ^2 defined as follows (see, e.g., [15]–[17]):

$$\chi^2 = \left[\ln R^s_{0.65}(\theta_0,\theta,\phi) - \ln R^t_{0.65}(\tau, D_e;\theta_0,\theta,\phi)\right]^2 + \left[\ln R^s_{1.64}(\theta_0,\theta,\phi) - \ln R^t_{1.64}(\tau, D_{\mathrm{e}};\theta_0,\theta,\phi)\right]^2 \quad (2)$$

where $R^s_{0.65}$ and $R^s_{1.64}$ are the simulated bidirectional reflectances at the 0.65- and 1.64-μm bands, respectively, and $R^t_{0.65}$ and $R^t_{1.64}$ are the bidirectional reflectances in the precalculated lookup table for ice clouds with a cloud geometrical thickness of 0.5 km and a cloud top height of 12 km. The present retrieval is carried out with $\theta_0 = 30°$, $\theta = 0°$, and $\phi = 90°$. The retrieved τ and D_{e} can then be obtained from the preceding minimization procedure.

Similar to the case for the IR-based retrieval, the relative errors in τ and D_{e} obtained on the basis of the solar bands are used to indicate the influence of the cloud geometrical thickness on the retrievals. The relative retrieval errors as a function of cloud reference τ are investigated (figure not shown). The errors in retrieved τ (less than 2%) are much smaller than their counterparts for the IR algorithm. An increase in cloud geometrical thickness results in a slight underestimation of the retrieved τ. Retrieval error increases with cloud geometrical thickness. The largest errors occur for large τ and small D_{e}. The sensitivity of errors to cloud top heights is very weak. The relative retrieval errors of D_{e} as a function of cloud reference D_{e} were also investigated (figure not shown). The errors are negligible except for very small values of D_{e}.

V. Conclusions and Discussion

In this paper, we investigate the effect of the ice cloud geometrical thickness on the retrieval of τ and D_{e} on the basis of algorithms using IR bands centered at 8.5 and 11 μm (or 12 μm) and solar bands centered at 0.65 and 1.64 μm (or 2.13 μm). We use the DISORT, a database of the ice cloud bulk single-scattering properties, and the correlated k-distribution routines for atmospheric gaseous absorption to simulate the IR brightness temperatures at 8.5, 11, and 12 μm and the solar reflectance functions at 0.65, 1.64, and 2.13 μm. In these simulations, the ice cloud top height is fixed at 12 or 15 km, but the cloud geometrical thickness varies from 0.5 to 5 km. The present simulations are carried out with $\theta = 0°$ for the IR bands and $\theta_0 = 30°$, $\theta = 0°$, and $\phi = 90°$ for the solar bands, respectively. The simulated brightness temperatures and reflectances are subsequently used to investigate the errors in the ice cloud τ and D_{e} retrieved from the precalculated lookup tables that assume a specific geometrical thickness (0.5 km). The variation of cloud geometrical thickness results in differences in the simulated brightness temperatures and bidirectional reflectances that in turn influence the retrievals. The effect of cloud geometrical thickness depends strongly on cloud τ for the IR retrieval, which, however, depends slightly on cloud D_{e}. The largest influence of cloud geometrical thickness is observed when τ is around 5 for the IR bands. In the nonabsorbing 0.65-μm band, the effect of the cloud geometrical thickness on reflectance increases with increasing τ and decreasing D_{e}. For the particle-absorbing bands (1.64 and 2.13 μm), the largest impact on the observed reflectance occurs when both τ and D_{e} are small.

Using the simulated results with a cloud geometrical thickness of 0.5 km as a reference, we developed lookup tables for inferring ice cloud τ and D_{e} using an 8.5- and 11-μm IR algorithm, and 0.65- and 1.64-μm solar reflectance algorithm. The lookup tables are then used for retrievals from the simulated IR brightness temperatures and solar bidirectional reflectances for cloud geometrical thicknesses of 1, 3, and 5 km.

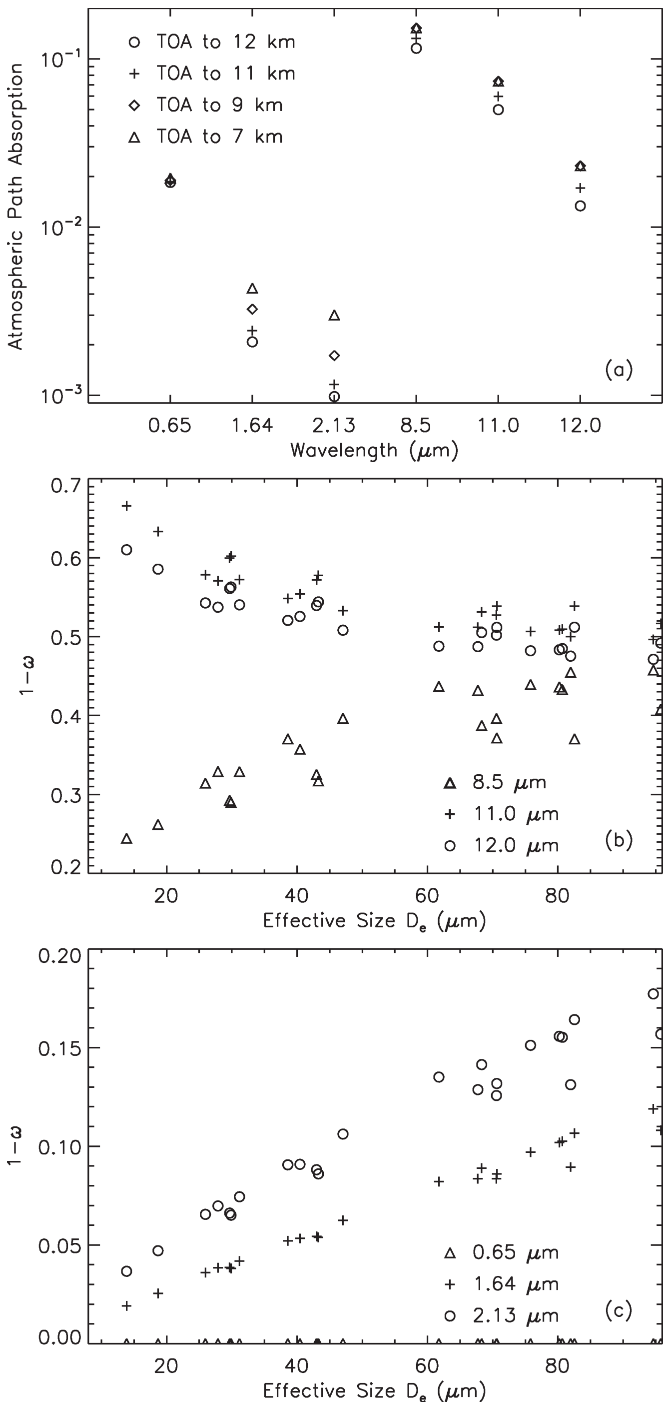

Fig. 8. (a) Atmospheric path absorption from the TOA to cloud base, and the ice particle absorption (1–ω) varying with ice particle effective size (D_e) for (b) IR and (c) solar bands.

The retrieval errors generally increase with increasing τ with the exception being the retrieval of D_e from the solar bands. The effect of cloud geometrical thickness on retrievals is much stronger for the IR bands than for the solar bands. The retrieval errors increase with increasing cloud geometrical thickness. Moreover, the increase of cloud geometrical thickness leads to an underestimation of τ and an overestimation of D_e for the methods based on both IR and solar bands.

The effect of the ice cloud geometrical thickness on the retrieval of ice cloud optical thickness and effective particle size stems from the combination of atmospheric gaseous absorption and ice particle absorption. Fig. 8(a) shows the atmospheric path absorption from the TOA to 12, 11, 9, and 7 km (cloud geometrical thickness equal to 0, 1, 3, and 5 km). Fig. 8(b) and (c) shows the ice particle absorption 1-ω (ω is the single-scattering albedo) for the ice particle size distributions in a range of 8–96 μm [36], [37].

With neither atmospheric gaseous absorption nor ice particle absorption, the variation of the ice cloud geometrical thickness would not affect the radiances at TOA for either IR or solar bands. Also, if there was no atmospheric gaseous absorption and the cloud temperature was constant, the variation of the ice cloud geometrical thicknesses would not affect the TOA radiances. However, the temperature does vary within ice clouds, especially those of significant vertical extent. Thus, the TOA radiances change with the vertical cloud profile even if there is no atmospheric gaseous absorption. For IR bands, both the atmospheric gaseous absorption and ice particle absorption are strong [Fig. 8(a) and (c)]. This is the reason that the retrievals of ice cloud optical thickness and particle effective size are influenced more by the changes in cloud geometrical thickness (Figs. 6 and 7). The ice particle absorption for the solar bands is much weaker than that for the IR bands. The atmospheric path absorption [Fig. 8(a)] at 1.64- and 2.13-μm bands is much weaker than for the IR bands. The 0.65-μm band has similar atmospheric path absorption as the 12-μm band, but it has nearly no ice particle absorption. Therefore, for the solar bands, the ice cloud geometrical thickness has a weak influence on the retrieval of the ice cloud optical thickness and particle effective size.

Cloud geometrical thickness can be inferred from satellite measurements of the cloud reflectance in the oxygen A-band [42]–[44] and solar reflection at 0.94-μm water vapor absorption band [45]. These methods based on solar reflection work only in the daytime. We intend to further explore the effect of the cloud geometrical thickness using active sensors such as lidar and radar. Techniques based on lidar have been used to estimate the cloud geometrical thicknesses with cloud τ less than two (see, e.g., [46]). Cloud radars can provide the vertical structure of clouds (see, e.g., [47]). The Cloud-Aerosol Lidar and Infrared Pathfinder Satellite Observation (CALIPSO), CloudSat, and Aqua satellites included in the NASA A-Train satellite constellation separately fly within about 1 min of each other. The radar measurements from CloudSat and the lidar measurements from CALIPSO can provide cloud geometrical thicknesses of ice clouds, which can be used for the retrieval of ice cloud τ and D_e using the IR or solar bands from the AIRS and MODIS aboard the Aqua platform.

REFERENCES

[1] K.-N. Liou, "Influence of cirrus clouds on weather and climate processes: A global perspective," *Mon. Weather Rev.*, vol. 114, no. 6, pp. 1167–1199, Jun. 1986.
[2] W. B. Rossow and R. A. Schiffer, "Advances in understanding clouds from ISCCP," *Bull. Amer. Meteorol. Soc.*, vol. 80, no. 11, pp. 2261–2287, Nov. 1999.
[3] D. P. Wylie and W. P. Menzel, "Eight years of high cloud statistics using HIRS," *J. Climate*, vol. 12, no. 1, pp. 170–184, Jan. 1999.

[4] A. E. Dessler and P. Yang, "The distribution of tropical thin cirrus clouds inferred from Terra MODIS data," *J. Climate*, vol. 16, no. 8, pp. 1241–1247, Apr. 2003.

[5] D. K. Lynch, K. Sassen, D. O. Starr, and G. Stephen, *Cirrus*. New York: Oxford Univ. Press, 2002, p. 480.

[6] G. L. Stephens, S.-C. Tsay, P. W. Stackhouse, Jr., and P. J. Flatau, "The relevance of the microphysical and radiative properties of cirrus clouds to climate and climate feedback," *J. Atmos. Sci.*, vol. 47, no. 14, pp. 1742–1753, 1990.

[7] P. Minnis, P. W. Heck, and D. Y. Young, "Inference of cirrus cloud properties using satellite-observed visible and infrared radiances. Part II: Verification of theoretical cirrus radiative properties," *J. Atmos. Sci.*, vol. 50, no. 9, pp. 1305–1322, May 1993.

[8] M. I. Mishchenko, W. B. Rossow, A. Macke, and A. A. Lacis, "Sensitivity of cirrus cloud albedo, bidirectional reflectance and optical thickness retrieval accuracy to ice particle shape," *J. Geophys. Res.*, vol. 101, no. D12, pp. 16 973–16 985, 1996.

[9] B. A. Baum, D. P. Kratz, P. Yang, S. C. Ou, Y.-X. Hu, P. F. Soulen, and S.-C. Tsay, "Remote sensing of cloud properties using MODIS airborne simulator imagery during SUCCESS 1. Data and models," *J. Geophys. Res.*, vol. 105, no. D9, pp. 11 767–11 780, 2000.

[10] P. Minnis, J. K. Ayers, R. Palikonda, and D. Phan, "Contrails, cirrus trends, and climate," *J. Climate*, vol. 17, no. 8, pp. 1671–1685, Apr. 2004.

[11] D. O'C. Starr, "A cirrus-cloud experiment: Intensive field observations planned for FIRE," *Bull. Amer. Meteorol. Soc.*, vol. 68, no. 2, pp. 119–124, Feb. 1987.

[12] O. B. Toon and R. C. Miake-Lye, "Subsonic aircraft: Contrail and cloud effects special study (SUCCESS)," *Geophys. Res. Lett.*, vol. 25, no. 8, pp. 1109–1112, 1998.

[13] M. Baker, "Cloud physics: Inside history on droplets," *Nature*, vol. 413, no. 6856, pp. 586–587, Oct. 2001.

[14] M. D. King, "Determination of the scaled optical thickness of clouds from reflected solar radiation measurements," *J. Atmos. Sci.*, vol. 44, no. 13, pp. 1734–1751, Jul. 1987.

[15] T. Nakajima and M. D. King, "Determination of the optical thickness and effective particle radius of clouds from reflected solar radiation measurements. Part I: Theory," *J. Atmos. Sci.*, vol. 47, no. 15, pp. 1878–1893, Aug. 1990.

[16] M. D. King, S.-C. Tsay, S. E. Plantick, M. Wang, and K.-N. Liou, *Cloud retrieval algorithms for MODIS: Optical thickness, effective particle radius, and thermodynamic phase*, 1997. MODIS Algorithm Theoretical Basis Document, No. ATBD-MOD-05.

[17] P. Rolland, K.-N. Liou, M. D. King, S.-C. Tsay, and G. M. McFarquhar, "Remote sensing of optical and microphysical properties of cirrus clouds using MODIS channels: Methodology and sensitivity to physical assumptions," *J. Geophys. Res.*, vol. 105, no. D9, pp. 11 721–11 738, 2000.

[18] S. Platnick, M. D. King, S. A. Ackerman, W. P. Menzel, B. A. Baum, J. C. Riédi, and R. A. Frey, "The MODIS cloud products: Algorithms and examples from Terra," *IEEE Trans. Geosci. Remote Sens.*, vol. 41, no. 2, pp. 459–473, Feb. 2003.

[19] M. D. King, W. P. Menzel, Y. J. Kaufman, D. Tanre, B.-C. Gao, S. Platnick, S. A. Ackerman, L. A. Remer, R. Pincus, and P. A. Hubanks, "Cloud and aerosol properties, precipitable water, and profiles of temperature and humidity from MODIS," *IEEE Trans. Geosci. Remote Sens.*, vol. 41, no. 2, pp. 442–458, 2003.

[20] C. J. Stubenrauch, R. Holz, A. Chédin, D. L. Mitchell, and A. J. Baran, "Retrieval of cirrus ice crystal sizes from 8.3 and 11.1 μm emissivities determined by the improved initialization inversion of TIROS-N Operational Vertical Sounder," *J. Geophys. Res.*, vol. 104, no. D24, pp. 31 793–31 808, 1999.

[21] G. Rädel, C. J. Stubenrauch, R. Holz, and D. L. Mitchell, "Retrieval of effective ice crystal size in the infrared: Sensitivity study and global measurements from the TIROS-N Operational Vertical Sounder," *J. Geophys. Res.*, vol. 108, no. D9, pp. 4281–4292, 2003.

[22] F. Parol, J. C. Buriez, G. Brogniez, and Y. Fouquart, "Information content of AVHRR channels 4 and 5 with respect to the effective radius of cirrus cloud particles," *J. Appl. Meteorol.*, vol. 24, no. 7, pp. 973–984, 1991.

[23] M. B. Gothe and H. Grassl, "Satellite remote sensing of the optical depth and mean crystal size of thin cirrus and contrails," *Theor. Appl. Climatol.*, vol. 48, no. 2/3, pp. 101–113, Jun. 1993.

[24] P. Minnis, K.-N. Liou, and Y. Takano, "Inference of cirrus cloud properties using satellite-observed visible and infrared radiances. Part I: Parameterization radiance fields," *J. Atmos. Sci.*, vol. 50, no. 9, pp. 1279–1304, May 1993.

[25] D. P. Duda and J. D. Spinhirne, "Split-window retrieval of particle size and optical depth in contrails located above horizontal inhomogeneous ice clouds," *Geophys. Res. Lett.*, vol. 23, no. 25, pp. 3711–3714, 1996.

[26] P. Rolland and K.-N. Liou, "Surface variability effects on the remote sensing of thin cirrus optical and microphysical properties," *J. Geophys. Res.*, vol. 106, no. D19, pp. 22 965–22 978, 2001.

[27] Q. Fu and W. B. Sun, "Retrieval of cirrus particle sizes using split-window technique: A sensitivity study," *J. Quant. Spectrosc. Radiat. Transfer*, vol. 70, no. 4–6, pp. 725–736, Aug. 2001.

[28] P. Yang, B.-C. Gao, B. A. Baum, W. J. Wiscombe, Y. X. Hu, S. L. Nasiri, P. F. Soulen, A. J. Heymsfield, G. M. McFarquhar, and L. M. Miloshevich, "Sensitivity of cirrus bidirectional reflectance to vertical inhomogeneity of ice crystal habits and size distributions for two moderate-resolution imaging spectroradiometer (MODIS) bands," *J. Geophys. Res.*, vol. 106, no. D15, pp. 17 267–17 292, 2001.

[29] P. Yang, H.-L. Wei, B. A. Baum, H.-L. Huang, A. J. Heymsfield, Y. X. Hu, B.-C. Gao, and D. D. Turner, "The spectral signature of mixed-phase clouds composed of nonspherical ice crystals and spherical liquid droplets in the terrestrial window region," *J. Quant. Spectrosc. Radiat. Transfer*, vol. 79/80, pp. 1171–1188, 2003.

[30] Y. Luo, S. K. Krueger, G. G. Mace, and K.-M. Xu, "Cirrus cloud properties from a cloud-resolving model simulation compared to cloud radar observations," *J. Atmos. Sci.*, vol. 60, no. 3, pp. 510–525, Feb. 2003.

[31] P. Yang, K.-N. Liou, K. Wyser, and D. Mitchell, "Parameterization of the scattering and absorption properties of individual ice crystals," *J. Geophys. Res.*, vol. 105, no. D4, pp. 4699–4718, 2000.

[32] P. Yang, H. Wei, H.-L. Huang, B. A. Baum, Y. X. Hu, G. W. Kattawar, M. I. Mishchenko, and Q. Fu, "Scattering and absorption property database for nonspherical ice particles in the near- through far-infrared spectral region," *Appl. Opt.*, vol. 44, no. 26, pp. 5512–5523, Sep. 2005.

[33] B. A. Baum, P. F. Soulen, K. I. Strabala, M. D. King, S. A. Ackerman, W. P. Menzel, and P. Yang, "Remote sensing of cloud properties using MODIS airborne simulator imagery during SUCCESS 2, cloud thermodynamic phase," *J. Geophys. Res.*, vol. 105, no. D9, pp. 11 781–11 792, 2000.

[34] M. D. King, S. Platnick, P. Yang, G. T. Arnold, M. A. Gray, J. C. Riedi, S. A. Ackerman, and K. N. Liou, "Remote sensing of liquid water and ice cloud optical thickness, and effective radius in the arctic: Application of air-borne multispectral MAS data," *J. Atmos. Ocean. Technol.*, vol. 21, no. 6, pp. 857–875, Jun. 2004.

[35] J. Lee, P. Yang, A. Dessler, B. A. Baum, and S. Platnick, "The influence of thermodynamic phase on the retrieval of mixed-phase cloud microphysical and optical properties in the visible and near-infrared region," *IEEE Geosci. Remote Sens. Lett.*, vol. 3, no. 3, pp. 287–291, Jul. 2006.

[36] Q. Fu, "An accurate parameterization of the solar radiative properties of cirrus clouds for climate models," *J. Climate*, vol. 9, no. 9, pp. 2058–2082, Sep. 1996.

[37] D. L. Mitchell, Y. Liu, and A. Macke, "Modeling cirrus clouds. Part II: Treatment of radiative properties," *J. Atmos. Sci.*, vol. 53, no. 20, pp. 2967–2988, Oct. 1996.

[38] D. P. Kratz, "The correlated k-distribution technique as applied to the AVHRR channels," *J. Quant. Spectrosc. Radiat. Transfer*, vol. 53, no. 5, pp. 501–517, May 1995.

[39] D. P. Kratz and F. G. Rose, "Accounting for molecular absorption within the spectral range of the CERES window channel," *J. Quant. Spectrosc. Radiat. Transfer*, vol. 61, no. 1, pp. 83–95, Jan. 1999.

[40] K. Stamnes, S.-C. Tsay, W. Wiscombe, and K. Jayaweera, "Numerical stable algorithm for discrete-ordinate-method radiative transfer in multiple scattering and emitting layered media," *Appl. Opt.*, vol. 27, no. 12, pp. 2502–2509, Jun. 1988.

[41] Z. Luo and W. B. Rossow, "Characterizing tropical cirrus life cycle, evolution, and interaction with upper-tropospheric water vapor using Lagrangian trajectory analysis of satellite observations," *J. Climate*, vol. 17, no. 23, pp. 4541–4563, Dec. 2004.

[42] V. V. Rozanov and A. A. Kokhanovsky, "Semianalytical cloud retrieval algorithm as applied to the cloud top altitude and the cloud geometrical thickness determination from top-of-atmosphere reflectance measurements in the oxygen A band," *J. Geophys. Res.*, vol. 109, no. D5, p. D05202, 2004.

[43] A. A. Kokhanovsky and V. V. Rozanov, "Cloud bottom altitude determination from a satellite," *IEEE Geosci. Remote Sens. Lett.*, vol. 2, no. 3, pp. 280–283, Jul. 2005.

[44] V. V. Rozanov and A. A. Kokhanovsky, "Determination of cloud geometrical thickness using backscattered solar light in a gaseous absorption band," *IEEE Geosci. Remote Sens. Lett.*, vol. 3, no. 2, pp. 250–253, Apr. 2006.

[45] T. Hayasaka, T. Nakajima, Y. Fujiyoshi, Y. Ishizaka, T. Takeda, and M. Tanaka, "Geometrical thickness, liquid water content, and radiative properties of stratocumulus clouds over the western North Pacific," *J. Appl. Meteorol.*, vol. 34, no. 2, pp. 460–470, 1995.

[46] R. F. Cahalan, M. McGill, J. Kolasinski, T. Várnai, and K. Yetzer, "THOR—Cloud thickness from offbeam lidar returns," *J. Atmos. Ocean. Technol.*, vol. 22, no. 6, pp. 605–627, 2005.

[47] G. L. Stephens *et al.*, "The CloudSat mission and the A-train: A new dimension of space-based observations of clouds and precipitation," *Bull. Amer. Meteorol. Soc.*, vol. 83, no. 12, pp. 1771–1790, Dec. 2002.

Gang Hong received the B.S. degree in atmospheric sciences from Nanjing Institute of Meteorology, Nanjing, China, in 1995 and the Ph.D. degree in environmental physics and remote sensing from University of Bremen, Bremen, Germany, in 2004.

Currently, he is a Research Associate with the Department of Atmospheric Sciences, Texas A&M University, College Station. His recent research focuses on retrieving ice cloud and aerosol properties and investigating radiative properties of clouds from the MODIS and AIRS measurements.

Dr. Hong is an Affiliate Member of the IEEE.

Ping Yang received the B.S. degree in theoretical physics and the M.S. degree in atmospheric physics from Lanzhou University and Lanzhou Institute of Plateau Atmospheric Physics, Chinese Academy of Sciences, Lanzhou, China, in 1985 and 1988, repectively, and the Ph.D. degree in meteorology from University of Utah, Salt Lake City, in 1995.

After graduation from the University of Utah, he remained there for two years, working as a Research Associate. Later, he was an Assistant Research Scientist with the University of California, Los Angeles, and an Associate Research Scientist with the Goddard Earth Sciences & Technologies Center, University of Maryland, Baltimore County. He is currently an Associate Professor with the Department of Atmospheric Sciences, Texas A&M University, College Station. His research interests cover the areas of remote sensing and radiative transfer. He has been actively conducting a research in the modeling of the optical and radiative properties of clouds and aerosols, in particular, cirrus clouds, and their applications to space-borne and ground-based remote sensing. He has coauthored more than 80 peer-reviewed publications. He serves as an Associate Editor for the *Journal of Atmospheric Sciences*, the *Journal of Quantitative Spectroscopy & Radiative Transfer*, and the *Journal of Applied Meteorology* and *Climatology*.

Dr. Yang is a member of the MODIS Science Team. He received the Best Paper Award from the Climate and Radiation Branch, NASA Goddard Space Center in 2000, the U.S. National Science Foundation CAREER Award in 2003, and the Dean's Distinguished Achievement Award for Faculty Research, College of Geosciences, Texas A&M University in 2004.

Hung-Lung Huang received the B.S. degree in atmospheric science from National Taiwan University, Taipei, Taiwan, R.O.C., in 1984 and the M.S. and Ph.D. degrees in meteorology from University of Wisconsin-Madison, Madison, in 1986 and 1989, respectively.

In 1989, he joined the Cooperative Institute for Meteorological Satellite Studies (CIMSS) in the Space Science and Engineering Center (SSEC), University of Wisconsin-Madison, where he is a Distinguished Scientist. He is an Adjunct Professor with Nanjing University of Information and Technology and a guest Chief Scientist of National Satellite Meteorological Center of China Meteorology Administration. His research interests include remote sensing in the areas of atmospheric sounding retrieval, information content analysis, satellite and aircraft high-spectral resolution sounding instrument data processing, polar orbiting direct broadcast processing package development, data compression, instrument design and performance analysis, cloud-clearing, cloud property characterization, synergistic imaging, and sounding data processing and algorithm development.

Dr. Huang is a member of the International Radiation Commission, a regional Editor of SPIE Journal of Applied Remote Sensing, the U.S. Director of China-America Cooperative Remote Sensing Center, Nanjing University of Information and Technology, the Cochair of International (A)TOVS Working Group, a science council member of CIMSS UW-Madison, and a council member of SSEC UW-Madison.

Bryan A. Baum received the B.S. degree in chemical engineering from Vanderbilt University, Nashville, TN, in 1978, the M.S. degree in chemical engineering from University of Colorado, Boulder, and the Ph.D. degree in atmospheric science from Georgia Institute of Technology, Atlanta, in 1985 and 1989, respectively.

In 2006, he joined the Space Science and Engineering Center, University of Wisconsin-Madison, as an Associate Scientist. Prior to this, he was a Senior Scientist with the NASA Langley Research Center for over 16 years. His research activities have focused on satellite, aircraft, and surface-based remote sensing of single-layered and multilayered cloud properties from multispectral and hyperspectral imager data. His recent research has focused on the development of ice cloud bulk scattering and absorption models at visible through far-infrared wavelengths.

Dr. Baum is a member of the MODIS Science Team.

Yongxiang Hu received the Ph.D. degree in atmospheric sciences from University of Alaska, Fairbanks, in 1994.

He is currently a Senior Research Scientist with the Radiation and Aerosols Branch, NASA Langley Research Center, Hampton, VA. He worked as a Postdoctoral Researcher with the College of William and Mary and as a Research Professor with Hampton University before he joined NASA in 1999. His research interests include radiative transfer, passive and active atmospheric remote sensing, and satellite onboard data analysis.

Steven Platnick received the B.S. degree in electrical engineering from Duke University, Durham, NC, in 1979, the M.S. degree in electrical engineering from University of California, Berkeley, in 1980, and the Ph.D. degree in atmospheric sciences from University of Arizona, Tucson, in 1991.

In January 2003, he joined the NASA Goddard Space Flight Center, Greenbelt, MD, and he is currently the Deputy Project Scientist of the NASA's Aqua satellite. Prior to this appointment, he was a Research Associate Professor with the Joint Center for Earth Systems Technology, University of Maryland, Baltimore County, a position he held from 1996 to 2002. He has been working in collaboration with the NASA Goddard Space Flight Center since 1993, and prior to that, he held engineering positions with Hewlett-Packard Co., for six years, as well as a National Research Council Resident Research Associate position with the NASA Ames Research Center. His research experience includes theoretical and experimental studies of satellite, aircraft, and ground-based cloud remote sensing, including applications to MODIS.

Dr. Platnick is a member of the MODIS Science Team.